A Fast and Hardware Mimicking Analytic CT Simulator

H Ghadiri, A Rahmim, *Senior Member, IEEE,* M B Shiran, H Soltanian-Zadeh, *Senior Member, IEEE* and M R Ay, *Member, IEEE*

***Abstract*– Different algorithms have been utilized for x-ray computed tomography (CT) simulation based on Monte Carlo technique, analytic calculation, or combination of them. Software packages based on Monte Carlo algorithm provide sophisticated calculations but the time consuming nature of them limits its applicability. Analytic calculation for CT simulation has been also evaluated in recent years. Due to ignoring basic physical processes, analytic methods have limited applications. In this study, a hardware mimicking algorithm has been developed to accurately model the CT imaging chain using analytic calculation. The model includes x-ray spectrum generation according to the pre-defined scanning protocol. The detector is designed to acquire the data either in integral or spectral modes. CT geometry can be used as parallel or fan beam with different sizes. Poisson noise model was applied to the acquired projection data. Varieties of projection-based computerized phantoms have been designed and implemented in the simulator. CT number and background noise of the simulated images have been compared with experimental data. On average, the relative difference between simulated and experimental HUs are 8.3%, 7.5%, and 8.0% for bone; 12.1%, 10.3%, and 7.8% for contrast agent; and 16.6%, 3.6%, and 5.2% for the background at 80 kVp/500 mAs, 120 kVp/250 mAs, and 140 kVp/125 mAs, respectively. The relative difference between simulated and experimental noise values vary between 2% to slightly less than 26%. For scanning and image generation with a computer equipped with Intel Core2 Quad CPU and 2.0 GB of RAM, the simulator takes about 32 seconds for generating a 512×512 single slice image when it is adjusted to acquire 900 projection angles with 20 mm slice thickness and 140kVp/200 mAs scanning protocol. The simulation time is independent of photon intensity.**

I. Introduction

A noticeable amount of research has done to improve the image quality in computed tomography (CT), as an essential diagnostic tool. Migrating from single-slice to multi-slice and from single-energy to dual- and multi-energy CT, as well as focusing on dose optimization all attest to ongoing advances in CT technology. From a research point of view, rapid enhancements in the CT technology underline a need for developing fast and accurate CT simulation packages. In research areas with target method development and image quality improvement, the ability to attain fast and accurate CT simulations is crucial. Different algorithms have been utilized for simulation of x-ray CT based on the Monte Carlo technique [1], analytic calculations [2], or a hybrid [3] of them. Although software packages based on the Monte Carlo approach provide sophisticated computations to model the real physical processes, the time consuming nature of them limit applicability in research wherein substantial sets of images must be generated. Analytic calculations for CT simulation have also been evaluated in recent years. Based on this approach, the stochastic nature of x-ray beam generation and attenuation is simplified to direct analytic calculation leading to acquisition of results more efficiently compared to Monte Carlo methods. However due to ignoring a number of physical processes, such analytic methods may have limited applications. As such, it is of high importance to develop a CT simulation package capable of accurately modeling the CT imaging chain in computationally feasible times. In this study, a CT simulation package has been designed and developed which mimics the clinical CT imaging chain.

H Ghadiri is with the Department of Medical Physics and Biomedical Engineering, and Research Center for Molecular and Cellular Imaging, Tehran University of Medical Sciences, Tehran, Iran.

A Rahmim is with the Department of Radiology and Radiological Science, Johns Hopkins University School of Medicine, Baltimore, Maryland, USA.

M B Shiran is with the Department of Medical Physics, Iran University of Medical Sciences, Tehran, Iran.

H Soltanian-Zadeh is with the Departments of Research Administration and Radiology, Henry Ford Hospital, Detroit, Michigan, USA and the School of Electrical and Computer Engineering, University of Tehran, Tehran, Iran.

M R Ay is with the Department of Medical Physics and Biomedical Engineering, and Research Center for Molecular and Cellular Imaging, Tehran University of Medical Sciences, Tehran, Iran.

II. Materials and Methods

A. Analytic Projection

The geometric projections are calculated around the computerized phantom (described later); with defined geometry and materials in customizable angular steps and customizable energy range (e.g., 1 to 140 keV with 1 keV steps). Using an arc detector consisting of 725 elements (consistent with a 512X512 image with 1-mm pixel size), designed for fan-beam geometry, the projections P(θ, t, E) are generated in 0.4 degree increments along full rotation (900 projections for 360 degrees). To generate geometric projection matrix *P,* we forward project all designed phantoms using:

$$P(\theta, t; E) = \int_{S(\theta,t)} \mu(x, y; E) dS \qquad (1)$$

where $\mu(x, y; E)$ is the two dimensional distribution of the linear attenuation coefficients (LAC) in one slice of the corresponding computerized phantom at energy E, while θ and t represent the projection angle and radial coordinate, respectively, along the ray path S. Thus, the generated projection matrix consists of 725x900 elements for each energy step. So, for each of the computerized phantoms, an

individual projection matrix is generated and saved as a computer file. As such, for computerized tomography procedure, these projection matrix files can be used to generate cross sectional images with various scanning parameters.

B. Analytic Data Acquisition

The user can customize the CT geometry as parallel or fan beam with arbitrary values such as source to iso-center and iso-center to detector distances, number of detector elements and fan-beam angle, as well as projection angles. The x-ray beam is analytically traversed through the object and the intensity and energy of the attenuated beam are registered in the detector channels, which are equipped with a customizable response function $f(E)$. Matrix-based calculation is used to speed up the simulation process. To generate detected signals in the detector, firstly, calculated initial x-ray spectrum is transmitted through the object and then the attenuated spectrum is registered. To perform the transmission and attenuation process, we have designed a novel algorithm, in which the projection matrix together with x-ray spectrum and detection efficiency are directly used in the formulation, as below,

$$I_d(\theta,t) = \sum_{E=E_{min}}^{E_{max}} f(E).w(E).I_0(E).e^{-P(\theta,t;E)} \qquad (2)$$

where $I_d(\theta,t)$ is a projection matrix in which each element is weighted summation of $e^{-P(\theta,t;E)}$ values on the $E_{min}$and E_{max} energy range, where the weights come from initial X-ray spectrum $I_0(E)$. This means that the calculations of the detected photon intensities are performed in the projection space by parallel calculation, which makes the simulation very fast. For this, the object under scanning is used as a projection matrix $P(\theta,t;E)$ defined using the angular and azimuthal coordinate system. Each element of this matrix is the line integral along the ray path directed through angle θ and crossing the detector element in the t azimuthal coordinate at energy E. The detection efficiency of the detector, ranging from 0% to 100%, as a function of energy is designated as $f(E)$. The energy weighting factor, which converts the energy of photons to the signal generated by the detector, is represented by $w(E)$, ranging from $w(E)=1$ to $w(E)=E$. $I_0(E)$ is described below.

C. Analytic X-ray Spectrum

One of the main aims of our modeling approach is to accurately simulate image noise and image quality, and therefore, in the model the quality and quantity of the x-ray spectrum is calculated based on essential physical parameters. To calculate the quality and quantity of the initial x-ray spectrum I_0, the following parameters are taken into account: x-ray tube total aluminum equivalent filtration x_{Al} (mm), collimator opening A (mm^2) (which varies with slice thickness), x-ray tube current-time mAs and potential kVp. By applying the general Beer-Lambert exponential attenuation function we derived the following formula:

$$I_0(E) = A.mAs.I_r(E).e^{-x_{Al}.\mu_{Al}(E)} \quad 1 \le E \le kVp \qquad (3)$$

where $I_r(E)$ is the discrete x-ray spectrum as intensity of photons in 1 keV steps of energy emitted from the focal spot (in counts per mAs.mm^2) obtained from IPEM report 78 [4]. $\mu_{Al}(E)$ is the LAC of aluminum at energy E derived from Ref. [5]. Since the total filtration of x-ray tube and HVL is generally mentioned in aluminum equivalent value by the manufacturers, we have used aluminum filter in order to accurately model the x-ray tube output to better simulate the commercial CT. The total filtration of x-ray tube is assumed as the sum of inherent and added filters. The result of above formula is a vector consisting of the number of x-ray photons for each energy step between E=1 to E=kVp in the unit of keV.

D. Analytic Detection System

The detector is designed such that it can acquire the data either in integral (current) or spectral (energy-sensitive) modes. For integral mode CT imaging, for example with 120 kVp tube potential, the values of $E_{min}=1$ keV and $E_{max}=120$ keV can be used in the Eq. (2) leading to integration on the whole transmitted spectrum. For this mode, one can use $w(E)=E$ to model the proportionality of detector signal with photon energy. In the spectral mode with energy binning capability, in which the transmitted photons is subdivided into multiple energy bins and counted, the $w(E)$ can be equal to 1 and for each energy bin the E_{min} and E_{max} are low and high thresholds of energy bins. When $w(E)=1$, the pure photon-counting detector would be simulated. Quantum noise fluctuation of detected signals can be simulated by invoking Poisson distribution with a mean of I_d as:

$$I_p = Poisson(I_d) \qquad (4)$$

where I_p is projection matrix with added Poisson noise. By considering the mean value of I_d in abovementioned Poisson function, inverse proportionality of quantum noise to the signal intensity would be realized. Since, the Poisson mean is determined by the value of each element of the $I_d(\theta,t)$ matrix, which in turn is determined by $I_0(E)$, it behaves very similar to what happens in a real detection system.

Another aim of our model is to accurately simulate the CT numbers. For this, a beam hardening correction (BHC) algorithm was also designed to correct the acquired projection data. A software procedure inside the simulator is used to measure the extent of beam hardening along the projections by using a water calibration procedure. To this end, a computerized cylindrical water phantom to obtain beam hardening correction factors has been designed. In this particular software procedure, in the smoothed reconstructed image of the water phantom, the rate of decrease in the pixel values moving from the edge to the center of water phantom was extracted. A first order linear least square fitting is used to generate a function which represents the profile intensity variation versus phantom depth. The slope and intercept of the obtained linear function was recorded in the calibration file. In the imaging procedure of the simulation program, these

parameters are used to correct beam hardening effects in the projection matrix as:

$$I = BHC(I_p) \quad (5)$$

where the BHC function returns the beam hardening corrected matrix of I_p as I. Therefore, matrix I is the corrected final sinogram, in which each element corresponds to one projection and one element of detector. For each CT parameter that may have different x-ray characteristics, such as x-ray tube filtration or kVp, an individual calibration file must be considered. The line integrals of the projections, Q, were calculated as below,

$$Q = \ln\frac{I_0}{I} \quad (6)$$

where I_0 is calculated from Eq. (2) when no object exists in the ray paths. Each element of the Q matrix (sinogram) is a line integral along a ray path. As such, Q can be transformed to the cross sectional image by image reconstruction algorithm, such as the conventional filtered-back-projection (FBP) algorithm. For image reconstruction, we used MATLAB (The MathWorks, Inc.) codes to reconstruct the Q line integrals as a 512x512 image size. It is obvious that in spectral mode CT, each energy bin has a corresponding line integral matrix Q, which can be reconstructed to bin images.

E. Computerized Phantoms

Varieties of shape-based computerized phantoms are designed during simulation. The phantoms are designed such that they consist of distribution of LACs of different materials filled in different geometrical shapes, designated as $\mu(x, y; E)$ (see Eq. (1)). Three important examples of our designed phantoms are: (i) a 250 mm diameter cylindrical phantom filled with water for water calibration and beam hardening correction; (ii) a cylindrical multi-contrast phantom with 12 cavities filled with different concentrations of bony and contrast materials; and (iii) an anthropomorphic abdomen phantom; (iv) an examiner phantom for simulation model validation. The attenuation coefficient data of materials and tissues used in the simulation are calculated by WinXcom software [5]. To calculate LAC of solutions $\mu_s(E)$ (such as K_2HPO_4 solution for bone modeling), we consider the following mixture rule:

$$\mu_S(E) = \rho_S . \sum_i w_i \sigma_i(E) \quad (7)$$

where w_i, and σ_i are the mass fraction and mass attenuation coefficient of the ith element in the solution. Alternatively, LAC of mixtures μ_M (such as diluted contrast agents when it is insoluble in water), the volume fraction-based formula is used as:

$$\mu_M(E) = \sum_i v_i \mu_i(E) \quad (8)$$

where v_i and μ_i are the volume fraction and LAC of contrast agent and water in the mixture.

F. Experimental Model Validation

We have validated our simulation model by comparing with experimental data on the physical phantom which has the same size and contents as the simulation phantom. Experimental and simulated images of the examiner phantom were acquired using a variety of tube potential (kVp) and current-time (mAs) combinations. Experimental and simulation results were compared for HU and noise values in ROIs defined over phantom images.

For experimental CT examinations we used a clinical integral mode 64-slice CT system (GE Healthcare, Milwaukee, WI, USA). All data acquisitions were performed following service calibration and image quality verification. All CT scans were acquired with 5mm slice thickness in the axial mode. Tube potentials for CT scanning were adjusted to 80, 120, and 140 kVp at various x-ray tube current-time values. For this, both the experimental and computerized examiner phantom cavities were filled with K_2HPO_4 and Visipaque320 (GE Healthcare, Inc) with same concentrations. CT images of the phantom obtained using the implemented simulation code were compared to those obtained from the experiments in all kVps and range of mAs for Hounsfield Unit (HU) and noise values over three types of regions: (1) those containing various K_2HPO_4 concentrations, (2) those with various concentrations of Visipaque320 (3) and those considered as background.

III. RESULTS

A. Noise and HU Accuracy of the Model

To assess the accuracy of HU calculation, mean of the HU values in all ROIs were calculated. To assess the statistical noise, standard deviations of the HU values in ROIs placed in the background were calculated and averaged. The HU assessment results for 80 and 140 kVp are shown in Fig. 1. On average, the percentage relative difference (RD%) between simulated and experimental HUs are 8.3, 7.5 and 8.0% for bone; 12.1, 10.3, and 7.8% for contrast agent; and 16.6, 3.6, and 5.2% for the background at 80 kVp/500 mAs, 120 kVp/250 mAs, and 140 kVp/125 mAs, respectively. The statistical noise assessment results for images acquired using different combinations of kVp and mAs values are summarized in Table I. The percentage relative difference between simulated and experimental noise values vary between 2% to slightly less than 26%. The same results (not shown) were obtained when repeating the same procedure for other possible combinations of kVp and mAs values.

B. Integral and Spectral CT Simulation

Both integral mode CT and spectral mode CT can be simulated by the developed simulator. In the Fig 2 generated images of anthropomorphic phantom by analytic model of CT with integral mode detector are shown. In this case some regions in the liver, stomach, and intestine have abnormal contrast agent uptake together with aorta filled with blood pool contrast agent. In the Fig 3 spectral mode CT images of multi-contrast phantom filled with three different contrast agents with three different concentrations, and bone are shown. In this case, the detector works in energy-sensitive mode, so the images are corresponding to different energy bins

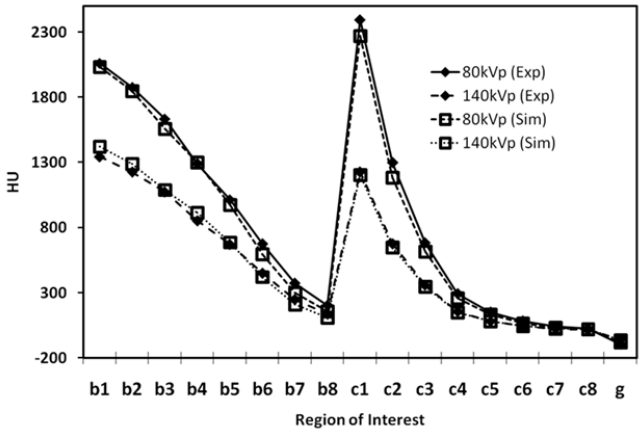

Fig 1. HU measurements of different ROIs within the test phantom images generated from experimental and simulated studies. The points are connected only to aid in separating the points and show the similarity of pattern of change in experimental and simulated data (not meant to represent inter-relation between points).

TABLE I. PERCENTAGE RELATIVE DIFFERENCE BETWEEN SIMULATED AND EXPERIMENTAL MEASUREMENTS OF NOISE IN CT IMAGES ACQUIRED AT DIFFERENT X-RAY TUBE kVp AND mAs.

kVp	mAs		
	500	250	125
80	15.5	17.4	20.0
120	2.0	15.7	25.3
140	4.9	6.9	15.6

.

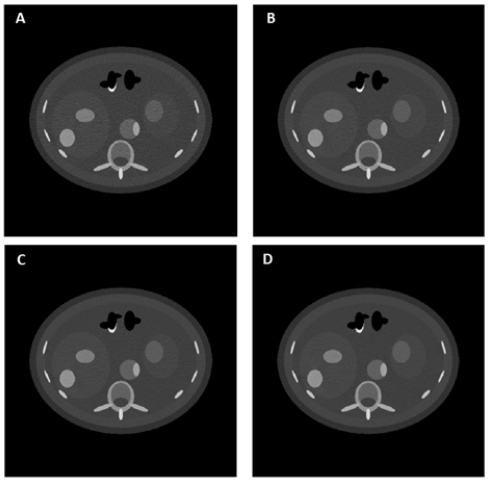

Fig 2. Generated images of anthropomorphic phantom by analytic model of CT with integral mode detector. A) 120 kVp, 10 mAs. B) 120 kVp, 20 mAs. C) 120 kVp, 30 mAs. D) 120 kVp, 40 mAs. Abnormal uptake of contrast agent in the liver, stomach, and intestine can be observed. Moreover, a calcification can be seen inside aorta containing blood pool contrast agent. (For all image WW=2000, WL=500).

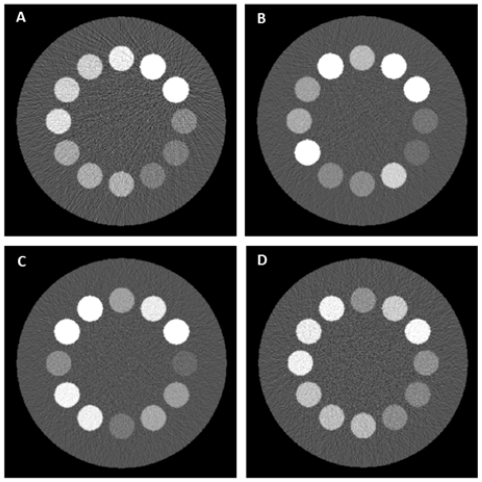

Fig 3. Generated images of multi-contrast phantom by analytic model of CT with spectral mode detector with 140kVp and 100mAs. A) bin=40-50 keV B) bin=51-65 keV. C) 66-80 keV. D) 81-90 keV. Positions 3, 4, 5 O'clock are filled with Gd concentrations, positions 6, 7, 8 O'clock with Hf concentrations, positions 9, 10, 11 O'clock with Au concentrations, and positions 12, 1, 2 O'clock are filled with bony material concentrations. (For all image WW=2000, WL=500).

C. Model Running Speed

Unlike to Monte Carlo-based simulation models, the needed time to both data and image generation is independent of photon intensity in our proposed analytical model.

Examining our simulator for measuring its speed for generating a 512×512 single slice image with data including 900 projections and 725 detector element for 120kVp/100 mAs scanning protocol, we observed that (i) the simulator takes about 32 seconds, when the computer equipped with Intel® Core™ 2-Quad CPU@2.0GHz and 2.00 GB of RAM run by 32-bit Microsoft Windows is used; (ii) it takes about 3.4 seconds, when the computer equipped with Intel® Core™ i7 CPU@2.20GHz and 8.0 GB of RAM run by 64-bit Microsoft Windows is used.

IV. DISCUSSION AND CONCLUSION

Availability of a CT simulator capable of taking into account different scanning parameters such as kVp, mAs, and slice thickness, such that accurate HU values is generated, can be very useful for research work related to protocol and dose optimization. Moreover, near-to-real noise mimicking behavior can extend its applications especially in research work that includes noise consideration such as reconstruction-based noise reduction. Straightforward design and customizable phantoms with capability of using any kind of solutions/mixtures in any place of phantoms seems to be promising for vast varieties of applications.

Independency of our model running time from the number of simulated photons together with dependency of image noise to the photons flux may help in applications in which large amounts of cross sectional images with different conditions should be generated.

Capability of our model to simulate energy-sensitive CT with ability for energy binning in the data acquisition system

part can help the researchers who are working on optimization and designing of the newly introduced concept, spectral CT. As an example, our analytic CT simulator has been recently utilized for development of multiple simultaneous contrast agents discrimination using spectral CT system [6].

In conclusion, we have designed and validated a fast and accurate CT simulator that mimics various physical phenomena in the course of CT acquisition. Ongoing efforts continue for further validation of this package and enhancement of noise accuracy, by modeling other affecting parameters, as well as improving image reconstruction algorithms.

REFERENCES

[1] M. Bazalova, and F. Verhaegen, "Monte Carlo simulation of a computed tomography x-ray tube," *Phys Med Biol,* vol. 52, no. 19, pp. 5945-55, Oct 7, 2007.

[2] W. P. Segars, M. Mahesh, T. J. Beck, E. C. Frey, and B. M. Tsui, "Realistic CT simulation using the 4D XCAT phantom," *Med Phys,* vol. 35, no. 8, pp. 3800-8, Aug, 2008.

[3] M. R. Ay, P. Ghafrain, and H. Zaidi, "A hybrid approach for fast simulation of X-ray computed tomography," in Nuclear Science Symposium Conference Record, 2007. NSS '07. IEEE, 2007, pp. 3155-3160.

[4] K. Cranley, B. J. Gilmore, G. W. A. Fogarty, L. Desponds, and D. Sutton, "Catalogue of diagnostic x-ray spectra and other data," *IPEM report,* vol. 78, 1997.

[5] L. Gerward, N. Guilbert, K. B. Jensen, and H. Levring, "WinXCom - a program for calculating X-ray attenuation coefficients," *Radiat Phys Chem,* vol. 71, no. 3-4, pp. 653-654, Oct-Nov, 2004.

[6] H. Ghadiri, M. R. Ay, M. B. Shiran, H. Soltanian-Zadeh, and H. Zaidi, "K-edge ratio method for identification of multiple nanoparticulate contrast agents by spectral CT imaging," *Br J Radiol,* vol. 86, no. 1029, pp. 20130308, Sep, 2013.